FEBS Letters 576 (2004) 306–312 FEBS 28855

Overexpression of AtHMA4 enhances root-to-shoot translocation of zinc and cadmium and plant metal tolerance

Frédéric Verret[a], Antoine Gravot[a], Pascaline Auroy[a], Nathalie Leonhardt[a], Pascale David[b], Laurent Nussaume[b], Alain Vavasseur[a], Pierre Richaud[a,*]

[a] *CEA Cadarache, DSV/DEVM/Laboratoire des Echanges Membranaires et Signalisation, UMR 6191 CNRS-CEA–Aix-Marseille II, F-13108 St Paul les Durance Cedex, France*
[b] *CEA Cadarache, DSV/DEVM/Laboratoire de Biologie du Développement des Plantes, UMR 6191 CNRS-CEA–Aix-Marseille II, F-13108 St Paul les Durance Cedex, France*

Received 11 May 2004; revised 6 September 2004; accepted 8 September 2004

Available online 25 September 2004

Edited by Julian Schroeder

Abstract AtHMA4 is an *Arabidopsis thaliana* P_{1B}-ATPase which transports Zn and Cd. Here, we demonstrate that AtHMA4 is localized at the plasma membrane and expressed in tissues surrounding the root vascular vessels. The ectopic overexpression of *AtHMA4* improved the root growth in the presence of toxic concentrations of Zn, Cd and Co. A null mutant exhibited a lower translocation of Zn and Cd from the roots to shoot. In contrast, the AtHMA4 overexpressing lines displayed an increase in the zinc and cadmium shoot content. Altogether, these results strongly indicate that AtHMA4 plays a role in metal loading in the xylem.

Keywords: AtHMA; Metal tolerance; P-type ATPase; Zn/Cd/Co; *Arabidopsis*

1. Introduction

Plants need essential micronutrients, including heavy metals such as Zn, Ni and Cu, for normal functioning of their metabolism. The uptake processes of these metal ions are not strictly selective. When present in excess, these and non-essential metals such as Cd, Pb, As and Hg are absorbed by roots and induce deleterious effects on various physiological processes (for review, see [1]). The distribution of these cationic elements in plants implicates transporters belonging to various families such as ABC, CDF, Nramp, and ZIP (for review, see [2,3]). One of these groups, the P_{1B}-ATPases, belongs to the large P-type ATPases superfamily, which are transporters that utilize the energy liberated from the exergonic ATP hydrolysis reaction in order to translocate positively charged substrates across membranes [4]. P_{1B}-ATPases are found in all living organisms, from archaea to humans and are thought to transport soft metal cations. They are referred to as HMAs [2,5] or CPx-type ATPases [2,6,7]. Genome sequences of two plants, *Arabidopsis thaliana* and *Oryza sativa*, both revealed eight genes belonging to the HMA group [8]. Compared with other eukaryotes, which only possess one or two P_{1B}-ATPases, the parallel expansion of the number of HMAs in *Arabidopsis* and *Oryza* suggests that these enzymes may play important roles in the movements of metals in plants. In *Arabidopsis*, based on full-length sequence alignments and intron positions [8], HMA1-4 and HMA5-8 were predicted to transport Zn/Cd/Pb/Co and Cu/Ag, respectively. The first two characterized enzymes are members of the Cu/Ag transport subgroup. AtHMA7 (RAN1) has been identified as a transporter delivering Cu^+ across post-Golgi membranes to create functional ethylene receptors [9,10]. AtHMA6 (PAA1) has been characterized as a Cu transporter, which participates in the translocation of this metal to chloroplastic copper proteins [11]. Until recently, members of the Zn/Cd/Pb/Co subgroup have only been characterized in prokaryotes [12–16]. First characterizations of plant homologs have recently been published [17–19]. Concerning AtHMA4, it has been shown that its expression confers Cd tolerance to *Saccharomyces cerevisiae* and restores Zn tolerance of the *Escherichia coli zntA* mutant, which is highly sensitive to this metal [17]. A more recent publication showed that an *hma2-2 hma4-1* double mutant presents a Zn nutritional deficiency phenotype and a decreased Zn content in shoots [18]. Using heterologous expression in yeast, we have demonstrated that AtHMA4 transports the four predicted metals (Zn/Cd/Pb/Co) [29]. Here, we describe the expression profile of *AtHMA4* from the Wassilewskija ecotype, its membrane localization and the effects of the deletion or overexpression on the plant metal content.

2. Materials and methods

2.1. Plant material and culture media

Plants were grown in a controlled-environment (8 h photoperiod of 300 μmol m^{-2} s^{-1}, 22 °C and 70% relative humidity), in a half strength MS medium [20], with additional 1% (w/v) sucrose and 0.7% (w/v) Bactoagar in the case of the solid medium. Germination of surface-sterilized seeds of *A. thaliana* wild-type Wassiliewskija (Ws), Columbia (Col-0), *hma4* mutant and *35S-HMA4* lines was performed on solid medium. After 2 weeks, the young plants were placed on sand for an additional 3 weeks period and finally transferred to an hydroponic culture system. Metals [$ZnSO_4$, $CdCl_2$, $Pb(CH3COO)_2$ and $CoCl_2$] were supplied at various concentrations as indicated in the figure legends.

* Corresponding author. Fax: +33-4-4225-2364.
E-mail address: pierre.richaud@cea.fr (P. Richaud).

Abbreviations: ICP-AES, inductively coupled plasma-atomic emission spectrometer; EGFP, enhanced green fluorescent protein

0014-5793/$22.00
doi:10.1016/j.febslet.2004.09.023

Table 1
Primers used for full-length cDNA cloning, expression level determination and T-DNA insertional mutant control

Name	Sequence
1HMA4	5′-CACTTCTCTCAACCTTTATCTGAT-3′
Rev14HMA4	5′-GTTATTCAATCAATCTCCATCAAG-3′
HMA4For230	5′-CGCAGCTTGCTTTACTGGGTATCAAGTGTT-GAAAG-3′
Rev2bisHMA4	5′-CATCTAAAACATTCCCTAGCTGTTCTTGAGC-3′
ACTIN8For	5′-GCACTTTCCAGCAGATGTGGATCTCTAAGGC-3′
ACTIN8Rev	5′- ACGCTGTAACCGGAAAGTTTCTCACATAGT-GCACAAATGAC -3′
9HMA4	5′-CCATTAAAAGGCCTAGGATCGACATC-3′
T-DNAgusRev1	5′-CCAGACTGAATGCCCACAGGCCGTC-3′
Rev18HMA4	5′-GCCTTTTGTGGAGCTAAGCTC-3′
10HMA4	5′-ATGGAGGCAGCAGCAGTTGTGTTCC-3′
Rev8HMA4	5′-GGGACAACCACTGACTAACACAAC-3′
Rev6HMA4	5′-GACCAATATGTTGATGTCGATCC-3′

Seeds of the *hma4* T-DNA insertional mutant, from the INRA Versailles collection, can be obtained under the reference DZO14h at www.dbsgap.versailles.inra.fr/publiclines/ and under the code number N9418 from the NASC library at www.arabidopsis.info/.

2.2. Cloning of the AtHMA4 cDNA

Total RNA was extracted from leaves of *A. thaliana* (Ws ecotype) according to [21]. *AtHMA4* full-length cDNA was amplified through RT-PCR using the ThermoScript™ RT-PCR system (Invitrogen™) and the Platinum® *Pfx* (Invitrogen™). Reverse transcription was performed using 4 μg total RNA and an oligo(dT)$_{20}$ primer. cDNA was amplified with the primer pair 1HMA4 and Rev14HMA4 designed on the Columbia genomic sequence At2g19110 (for primer sequences, see Table 1). The cDNA was cloned in the pCR®-XL-TOPO vector (Invitrogen™) and sequenced.

2.3. Analysis of AtHMA4 expression profile

RT-PCR. Total RNA was extracted from various tissues (roots, leaves, stems, cauline leaves, flowers and siliques) according to [21] and RT were carried out as described above. PCR were performed using the primers HMA4For230 and Rev2bisHMA4 [94 °C 3 min, then 94 °C 30 s/53 °C 30 s/68 °C 30 s]. *ACTIN8* gene was used as control on the same cDNA sample. The experiments were triplicated on independently isolated material.

Three RT-PCR were carried out to control the *hma4* mutant line, with primer pairs located upstream, on both sides and downstream relative to the T-DNA insertion position. The RT was carried out with the gene specific primer Rev6HMA4 for the first one; the first strand cDNA was used in PCR with the primers 1HMA4 and Rev6HMA4. The PCRs for the other two were performed with oligo(dT)$_{20}$ cDNA using primer pairs 1HMA4/Rev18HMA4 and 10HMA4/Rev8HMA4, respectively.

GUS activity. Plants or organs at different stages of their development were examined for GUS activity according to [22]. The samples were vacuum-infiltrated in the GUS staining solution (50 mM $NaPO_4$, pH 7.0, 0.01% (w/v) Triton X-100, 1 mM $K_3Fe(CN)_6$, 1 mM $K_4Fe(CN)_6$ and 1 mg ml^{-1} 5-bromo-4-chloro-3-indolyl-β-D-glucuronide (X-Gluc)), and incubated at 37 °C for 6 h. Pigments were then washed by incubation of stained samples in 70% (v/v) ethanol at 60 °C for 2 h. To perform transverse sections, plantlet roots were fixed in resin after dessication by successive ethanol baths of rising concentrations, for 30 min each.

2.4. Transient expression assays

After digestion by *Eco*RV, the CaMV35S cassette was subcloned in the *Eco*RV/*Stu*I sites of the pGreen0179 binary vector, giving the pVF90 clone. Protoplasts of *A. thaliana* mesophyll cells were isolated and transfected with the cDNAs of the C-ter translational fusion of AtHMA4::EGFP or the enhanced green fluorescent protein (EGFP) alone cloned in the *Eco*RI site of the vector pVF90 described above, by the polyethylene glycol method previously described [23,24]. Typically, 0.1 ml of protoplast suspension (2×10^5 ml^{-1}) was transfected with 30–50 μg of cDNA in the presence of 40% PEG (w/v) for 30 min at 23 °C. They were then washed with W5 solution (150 mM NaCl ; 125 mM $CaCl_2$; 5 mM KCl; 5 mM glucose and 1.5 mM MES–KOH, pH 5.6) and incubated in W5 solution overnight at 17 °C before observations. Transient expression experiments were repeated three times. EGFP excitation and emission were performed at 475 and 510 nm, respectively. Observations were carried out at a magnification of 64× (Leica). The EGFP fluorescence was monitored with a color camera (Diagnostic Instrument) and analyzed with the Spot software.

2.5. Obtention of AtHMA4 overexpressing lines

A *Sma*I site was added at the 3′-end of AtHMA4 by cloning the reverse-complementary primer pairs TopoFV1for (5′-GGCCG *CCCGGG*ATCCGGTACCACTAGTGAATTCGTCGACGA-3′) and TopoFV1rev in the *Not*I site of the pCR®-XL-TOPO vector. The cDNA of AtHMA4 was then extracted by *Bam*HI/*Sma*I digestion and cloned at the same sites in the pVF90 vector described above. This construction was introduced by electroporation in AGL1 cells of *Agrobacterium tumefaciens*. The agrotransformation of Col-0 plants was carried out by the floral dip method [25]. The transformant plants were selected on solid medium supplemented with hygromycin B (30 μg/ml).

2.6. ICP experiments

Hydroponically grown plants were harvested after 24 h of metal treatment. Leaves were dried for 48 h at 50 °C and mineralized. The metal content was determined using inductively coupled plasma-atomic emission spectrometer ICP-AES (Vista MPX, Varian SA).

3. Results

3.1. Cloning and sequence analysis of AtHMA4 from the Ws ecotype

Our study was conducted on the Wassiliewskija ecotype (Ws), since a T-DNA insertional mutant of *AtHMA4* was identified in the INRA Versailles collection. The full-length cDNA (3618 bp) was obtained by a two step RT-PCR performed with total RNA extracted from leaves, then cloned in the pCR®-XL-TOPO vector and confirmed by sequencing. By comparison with the sequence of the BAC At2g19110 from the Col-0 ecotype, only four base changes were detected, resulting in aa differences (H vs. Q in position 537; K vs. R in 805; N vs. T in 970 and K vs. T in 1056).

3.2. Tissue-specific expression of AtHMA4

The level of expression of *AtHMA4* in various organs of plants from the Ws ecotype was investigated by RT-PCR. The *AtHMA4* transcript was detected in all tissues analyzed with higher expression levels in roots, stems and more particularly in flowers (Fig. 1).

3.3. GUS expression

In the *hma4* mutant line, a T-DNA is inserted in the third intron (Fig. 2A). Southern hybridization with a probe corresponding to a fragment of the *GUS* gene showed that this insertion is unique. The PCR analysis, using a pair of primers designed on *AtHMA4* (9HMA4) and in the *GUS* gene of the T-DNA, demonstrated that the mutant line is homozygous for the insertion (data not shown). The absence of an *AtHMA4* transcript was verified by RT-PCR, using two different oligo-

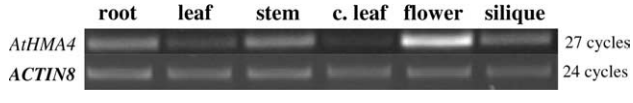

Fig. 1. Expression profile of *AtHMA4* determined by RT-PCR on RNA extracted from various tissues. Part of the *ACTIN8* transcript was used as a control.

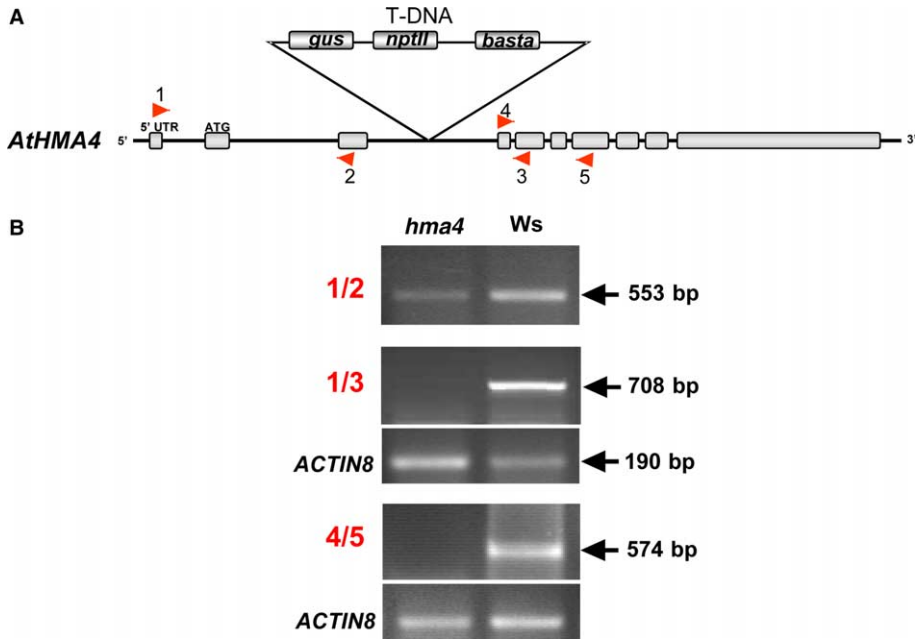

Fig. 2. (A) Exon/intron map of *AtHMA4* including the 5′ UTR and position of the T-DNA insertion in the *hma4* mutant. The red arrows indicate the different primers used for RT-PCR, using RNA extracts from *hma4* and Ws. (B) The T-DNA insertional *hma4* line is a knockout mutant for *AtHMA4*. The RT-PCR were carried out on RNA with different primer pairs, specific to *AtHMA4*. Upper: oligonucleotides 1 (1HMA4) and 2 (Rev6HMA4); middle: 1 and 3 (Rev18HMA4); bottom: 4 (10HMA4) and 5 (Rev8HMA4).

nucleotide pairs positioned downstream and at both sides of the insertion, respectively. The RT-PCR with wild-type Ws RNA extract yielded two amplification fragments of 708 bp and 574 bp when 1HMA4/Rev18HMA4 and 10HMA4/Rev8HMA4 primer pairs were used, respectively. These fragments were absent when *hma4* RNA extracts were used (Fig. 2B, middle and bottom parts). Interestingly, the *hma4* mutant presents a translational fusion of the *GUS* gene with

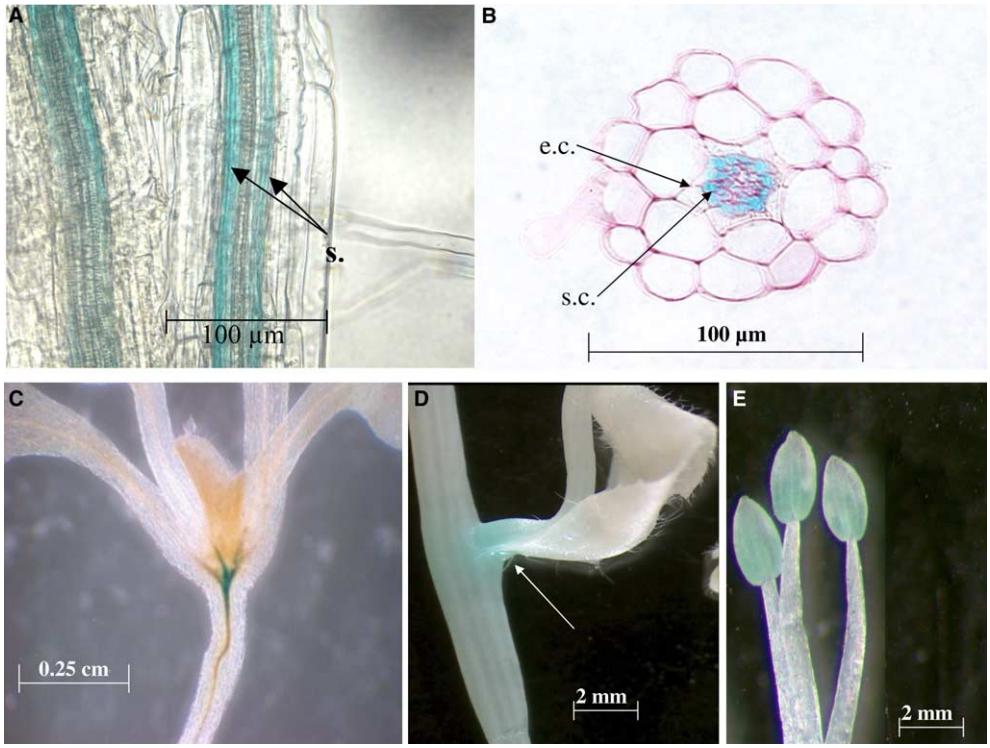

Fig. 3. Expression profile of AtHMA4 in planta revealed by GUS activity. (A) Roots (s.: stele); (B) root section (e.c.: endodermis cells; s.c.:stellar cells); (C) plantlet; (D) stem and cauline leaf; (E) stamens.

the two first exons of *AtHMA4*. Fig. 2B (upper part) shows a RT-PCR result using a primer pair located upstream of the insertion. In this case, the reverse transcription reaction was performed with the gene specific primer Rev6HMA4. An amplification fragment was observed with Ws and *hma4* RNA, confirming the existence of a transcript corresponding to the first two exons of *AtHMA4* and the *GUS* gene. This fusion allows detection of GUS activity under the control of the *AtHMA4* promoter. GUS staining was observed in roots, around the phloem and xylem vessels, whatever the state of development of the plant (from 4 days-old seedlings until 8 weeks-old plant) (Fig. 3A). In roots, GUS expression was particularly intense in stellar cells (Fig. 3B), in agreement with the results obtained by Birnbaum et al. [26]. A GUS staining was also observed in the vascular tissues under the shoot apical meristem, in the anthers and at the bases of cauline leaves (Fig. 3C–E). These results are in good agreement with those obtained by RT-PCR (Fig. 1) and the GUS profile presented in Hussain et al. [18].

3.4. Transient expression of AtHMA4 in mesophyll protoplasts

To investigate the localization of AtHMA4 protein at the subcellular level in planta, a C-ter translational fusion with the EGFP was constructed under the control of the CaMV35S promoter and transfected in protoplasts of mesophyll cells by the modified polyethylene glycol method [23,24]. In control cells expressing the EGFP alone, a diffuse fluorescence was observed in the cytoplasm and in the nucleus (Fig. 4B). Fig. 4C and D presents the protoplasts transfected with HMA4 fused in frame with the EGFP. The arrow in Fig. 4C indicates the vacuolar membrane peeled off from the plasma membrane. This result strongly suggests that AtHMA4 is localized at the plasma membrane of the protoplasts (Fig. 4D).

3.5. Deletion or overexpression of AtHMA4

To test the role of *AtHMA4* in *Arabidopsis*, we have used null mutant, overexpressing and wild-type plants, cultivated in hydroponic conditions for 24 h in the presence or absence of added metals and the metal content was determined in their leaves and roots (Fig. 5).

Leaves of *hma4* exhibited a lesser Zn or Cd content than the wild-type ones (Fig. 5A, left panel). Moreover, the metal content in roots was found higher in the deletion mutant (Fig. 5A, right panel).

To generate plants ectopically overexpressing AtHMA4, the cDNA was cloned under the control of the strong constitutive CaMV35S promoter and introduced in *Arabidopsis* through *A. tumefaciens*-mediated transformation. Two independent lines with elevated *AtHMA4* mRNA levels (controlled by RT-PCR, data not shown) carrying single T-DNA insertion were selected and self-crossed to obtain stable homozygous lines (seeds of these both lines can be obtained from the NASC library under the code numbers N9416 and N9417 at www.arabidopsis.info/). Leaves of AtHMA4 overexpressing plants significantly accumulated more Zn than the control (Fig. 5B, left panel). This was also the case for Cd at a con-

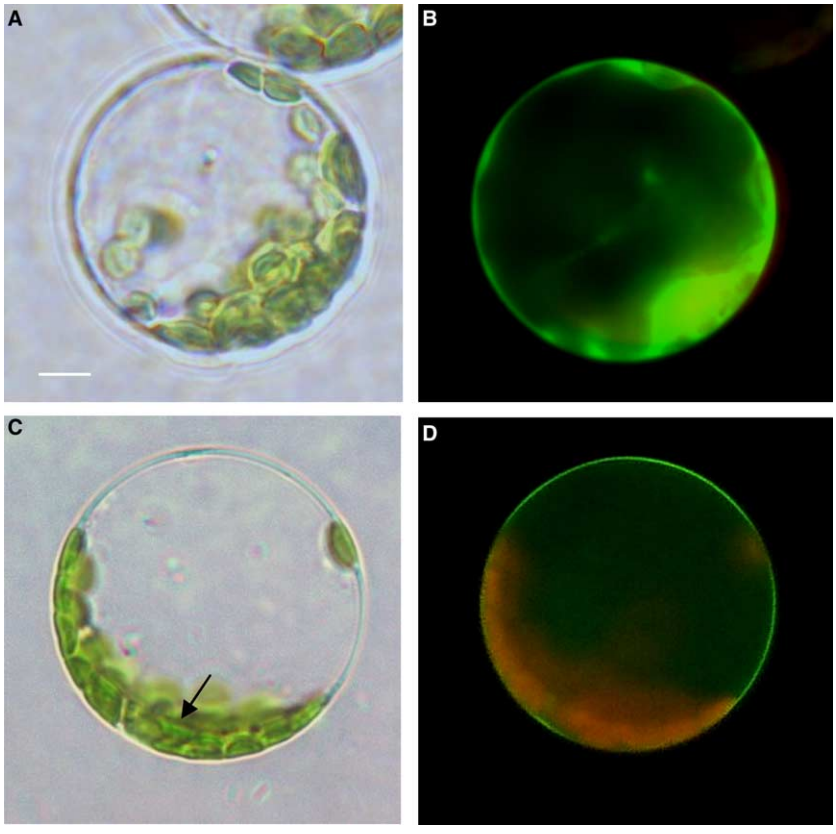

Fig. 4. Transient expression of the AtHMA4::EGFP chimeric protein fusion in transfected protoplasts of mesophyll cells. (A, B) Mesophyll protoplasts transfected with the EGFP cloned in pVF90 (A: transmission; B: GFP fluorescence); (C,D) mesophyll protoplasts transfected with the AtHMA4::EGFP construction (C: transmission; D: GFP fluorescence). In each case, protoplasts (0.1 ml) were transfected with 30–50 μg DNA. Bar = 5 μm. The red fluorescence observed in (D) corresponds to the autofluorescence of chlorophyll.

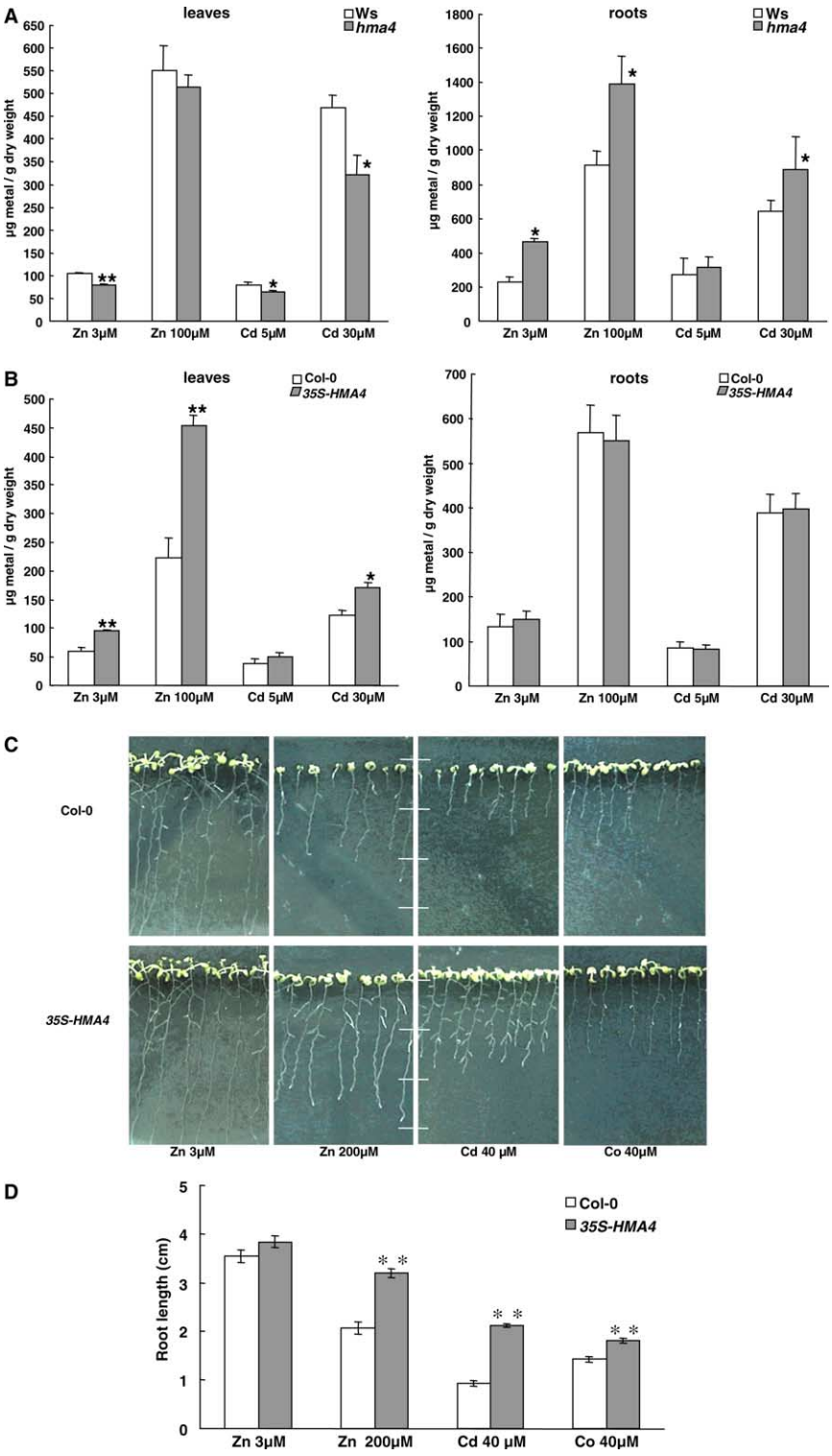

Fig. 5. Metal content and tolerance of wild-type (Col-0 or Ws), *35S-HMA4* overexpressing and *hma4* mutant plants. (A,B) Plants were hydroponically grown in the presence or absence (Zn 3 μM) of added metals during 24 h. Leaves and roots were harvested, dried, mineralized and the metal content determined by ICP-AES measurements. Values are means of six measurements ± S.E. Significant differences from the wild-type as determined by the Student's *t* test are indicated by one ($P < 0.05$) or two asterisks ($P < 0.001$). (C) Root length of vertically grown plantlets in the presence of the indicated concentrations of metals. Photographs of plates were realized 15 days after germination. (D) Root length measurements. Values are means of about 50 root length measurements ± S.E. The significant differences are indicated as described above ($P < 0.005$). The white horizontal bar scale = 1 cm.

centration of 30 μM. However, the metal contents in the roots were quite the same for wild-type and the overexpressing plants (Fig. 5B, right panel). Root growth measurements showed that the AtHMA4 overexpressing lines displayed increased Zn, Cd and Co tolerance (Fig. 5C and D). On control solid medium (nutrient solution containing Zn 3 μM), root

lengths of the overexpressing plants were identical to the ones of the wild-type plants. In contrast, on media containing high metal concentrations (Zn 200 μM, Cd 40 μM or Co 40 μM), the root lengths from overexpressing lines were longer by 55%, 128% and 27.5% compared to the wild-type root lengths, respectively. Shoots of overexpressing lines also presented a slight but significantly better development, in the presence of heavy metals, than the control ones (Fig. 5C).

4. Discussion

4.1. Expression pattern and localization of AtHMA4

In the present study, AtHMA4 expression pattern was determined in the Ws ecotype by RT-PCR and GUS activity. *AtHMA4* was found in all tested tissues, predominantly in roots, stems and flowers (Fig. 1). GUS observations of roots (intact tissue and transverse cuts) revealed that AtHMA4 is exclusively expressed in the stellar cells, the tissues surrounding the vascular vessels (Fig. 3A and B). This finding is corroborated by the predominant expression of *AtHMA4* in the stellar cells determined by microarray experiments [26]. In inflorescences, only the anthers presented a GUS activity (Fig. 3E). At the cellular level, AtHMA4::EGFP fusion transient expression in protoplasts of mesophyll cells strongly suggest that AtHMA4 is localized in planta at the plasma membrane (Fig. 4). It has been shown that AtHMA2 is also localized at the plasma membrane of plant cells [18]. The finding that AtHMA2 and AtHMA4 – which have the most related sequences in the HMA cluster – exhibit rather similar tissue expression patterns and the same membrane localization suggests some redundancy in the functions of these two transporters. Other transporters such as BOR1 and PHO1 involved in the xylem loading of boron and phosphate, respectively, display a very similar expression pattern in roots [27,28]. Altogether, these observations suggest a role for AtHMA4 in the loading/unloading of metals in the xylem (notably Zn), as proposed by Hussain et al. [18]. In roots, AtHMA4 could efflux metal from the stellar cells, inducing the loading of the xylem; in flowers, AtHMA4 could participate to the Zn nutrition of pollen grains at the level of the tapetum cells [18].

4.2. hma4 mutant characterization

hma4 plants did not present any obvious macroscopic phenotype. Nevertheless, the leaf metal content of the defective mutant was decreased in comparison to the one found with the wild-type plants (Fig. 5A, left panel), in agreement with Hussain et al. [18]. This result and the fact that only the double mutant *hma2-2 hma4-1* displays an obvious phenotype support our proposal for the role of AtHMA4. In *hma4* mutant plants, the translocation of metal from roots to shoot could be impaired. Moreover, the metal level in roots was found higher in *hma4* than in the wild-type, as expected in the presence of non-limiting metal concentrations in the nutrient solution and an unchanged metal root absorption process.

4.3. Overexpression of AtHMA4 enhances both the root-to-shoot metal translocation and the plant tolerance to Zn/Cd/Co

Ectopic overexpression of AtHMA4 *in planta* led to an increased tolerance to Zn, Cd and Co (Fig. 5C). This phenomenon is particularly obvious at the level of the root development. For example, in the presence of 40 μM Cd, the primary roots were two times longer and the secondary roots were well developed for the overexpressing lines compared to those of the wild-type plants. Metal content determination demonstrated that the overexpressing lines, when exposed to toxic concentrations of Zn or Cd, translocated these metals at a greater extent in the shoot, compared to the control plants (Fig. 5B, left panel). In contrast, the metal level was found rather similar in roots, indicating that the metal absorption by the roots compensates for the increased metal translocation to the shoot. The apparent discrepancy (both enhanced accumulation and tolerance) can be solved considering that the shoot represents the major part of the *Arabidopsis* biomass. The shoot exhibits large apoplastic and vacuolar compartments, which are potential metal sequestration compartments. Ectopic overexpression of AtHMA4 probably leads to an enhanced cellular metal efflux towards root and shoot apoplasts. In roots, this could result in the enhancement of metal loading in the xylem. In shoots, it could contribute to enhanced metal sequestration in the cell wall. Together, these phenomena could contribute to maintain low Zn/Cd/Co contents in the plant symplast, specially in roots. This hypothesis is in accordance with the increased sensitivity to Cd observed in the double mutant *cad1-3 hma4-1* [18], which is also impaired in the phytochelatin synthesis. This phenotype could result from Cd accumulation in root symplast, leading to a drastic impairment of plant growth.

Enhancement of root-to-shoot metal translocation is a major goal in phytoremediation [2]. In this context, AtHMA4, and probably also AtHMA2, could constitute interesting biotechnological tools.

Acknowledgements: This work was supported by the Commissariat à l'Energie Atomique (CEA) and the Toxicologie Nucléaire program of the CEA. We thank Serge Chiarenza for helpful technical assistance in preparation of root cuts and GUS observations and Nicole Bechtold and Matthieu Simon (INRA-Versailles, Station de Génétique et d'Amélioration des Plantes) for seeds of the T-DNA insertional *hma4* mutant. The authors acknowledge Drs. Phil Mullineaux and Roger Hellens for the pGreen0179 vector.

References

[1] Heavy Metal Stress in Plants (1999) (Prasad, M.N. and Hagenmeyer, J., Eds.) Springer-Verlag, Berlin, Heidelberg, New York.
[2] Williams, L.E., Pittman, J.K. and Hall, J.L. (2000) Biochim. Biophys. Acta 1465, 104–126.
[3] Clemens, S. (2001) Planta 212, 475–486.
[4] Inesi, G. (1985) Annu. Rev. Physiol. 47, 573–601.
[5] Axelsen, K.B. and Palmgren, M.G. (2001) Plant Physiol. 126, 696–706.
[6] Solioz, M. and Vulpe, C. (1996) Trends Biochem. Sci. 21, 237–241.
[7] Rensing, C., Mitra, B. and Rosen, B.P. (1997) Proc. Natl. Acad. Sci. USA 94, 14326–14331.
[8] Baxter, I., Tchieu, J., Sussman, M.R., Boutry, M., Palmgren, M.G., Gribskov, M., Harper, J.F. and Axelsen, K.B. (2003) Plant Physiol. 132, 618–628.
[9] Hirayama, T., Kieber, J.J., Hirayama, N., Kogan, M., Guzman, P., Nourizadeh, S., Alonso, J.M., Dailey, W. and Dancis, A. (1999) Cell 97, 383–393.
[10] Woeste, K.E. and Kieber, J.J. (2000) Plant Cell 12, 443–455.
[11] Shikanai, T., Müller-Moulé, P., Munekage, Y., Niyogi, K.K. and Pilon, M. (2003) Plant Cell 15, 1333–1346.
[12] Lebrun, M., Audurier, A. and Cossart, P. (1994) J. Bacteriol. 176, 3040–3048.
[13] Lebrun, M., Audurier, A. and Cossart, P. (1994) J. Bacteriol. 176, 3049–3061.

[14] Rensing, C., Sun, Y., Mitra, B. and Rosen, B.P. (1998) J. Biol. Chem. 273, 32614–32617.
[15] Tsai, K.-J., Lin, Y.-F., Wong, M.D., Yang, H.H.-C., Fu, H.-L. and Rosen, B.P. (2002) J. Bioenerg. Biomemb. 34, 147–156.
[16] Hou, Z. and Mitra, B. (2003) J. Biol. Chem. 278, 28455–28461.
[17] Mills, R.F., Krijger, G.C., Baccarini, P.J., Hall, J.L. and Williams, L.E. (2003) Plant J. 35, 164–176.
[18] Hussain, D., Hazydon, M.J., Wang, Y., Wong, E., Sherson, S.M., Young, J., Camakaris, J., Harper, J.F. and Cobbett, C.S. (2004) Plant Cell 16, 1327–1339.
[19] Gravot, A., Lieutaud, A., Verret, F., Auroy, P., Vavasseur, A. and Richaud, P. (2004) FEBS Lett. 561, 22–28.
[20] Murashige, T. and Skoog, F. (1962) Physiol. Plant 15, 473–497.
[21] Verwoerd, T.C., Dekker, B.M. and Hoekema, A. (1989) Nucleic Acids Res. 17, 2362.
[22] Jefferson, R.A., Kavanagh, T.A. and Bevan, M.W. (1987) EMBO J. 6, 3901–3907.
[23] Kovtun, Y., Chiu, W.-L., Tena, G. and Sheen, J. (2000) Proc. Natl. Acad. Sci. USA 97, 2940–2945.
[24] Clough, S.J. and Bent, A.F. (1998) Plant J. 16, 735–743.
[25] Abel, S. and Theologis, A. (1995) Plant J. 8, 87–96.
[26] Birnbaum, K., Shasha, D.E., Wang, J.Y., Jung, J.W., Lambert, G.M., Galbraith, D.W. and Benfey, P.N. (2003) Science 302, 1956–1960.
[27] Takano, J., Noguchi, K., Yasumori, M., Kobayashi, M., Gajdos, Z., Miwa, K., Hayashi, H., Yoneyama, T. and Fujiwara, T. (2002) Nature 420, 337–340.
[28] Hamburger, D., Rezzonico, E., MacDonald-Comber Petétot, J., Somerville, C. and Poirier, Y. (2002) Plant Cell 14, 889–902.
[29] Verret, F., Gravot, A., Auroy, P., Preveral, S., Forestier, C., Vavasseur, A. and Richaud, P. Heavy metal transport by ATHMA4 involves the N-ter degenerated HMA domain and the C-ter His11 stretch (submitted).